

MAPPING OF TAIGA FOREST UNITS USING AIRSAR DATA AND/OR OPTICAL DATA, AND RETRIEVAL OF FOREST PARAMETERS

Eric Rignot, Cynthia Williams[†], and Jo Bea Way.

Jet Propulsion Laboratory, California Institute of Technology, Pasadena CA 91109

[†]Institute of Northern Forestry, U.S. Forest Service, Fairbanks, AK 99701 USA

ABSTRACT

A maximum a posteriori Bayesian classifier is used to perform a supervised classification of multifrequency, polarimetric, airborne, SAR observations of boreal forests from the Bonanza Creek Experimental Forest, near Fairbanks, AK, into six categories: 1) white spruce; 2) black spruce; 3) balsam poplar; 4) alder; 5) treeless areas; and 6) open water. Tree classification accuracy is highest (86%) using L- and C-band fully polarimetric combined on a date where the forest just recovered from river flooding. The SAR map compares favorably with a vegetation map obtained from digitized aerial infra-red photos. C-band frequency and HV-polarization are, respectively, the most useful frequency and polarization for mapping tree types using SAR. Combination of multi-date SAR observations does not improve classification accuracy, and SAR data acquired on different dates, under different environmental conditions, yield classification accuracies 16% to 41% lower. Single-frequency, single-polarization, SAR data show limited mapping capability. Multispectral SPOT observations of the same area on a single date yield a classification accuracy of 78%. Combining optical and SAR data is useful for identifying tree species, independent of ground truth verification, using biomass estimates from SAR at L-band HV-polarization, NDVI from SPOT red and infra-red radiances, and an unsupervised segmentation map of the SAR data.

INTRODUCTION

Mapping tree species using remote sensing techniques is important for forest monitoring, and for improving estimates of regional, continental, and global photo-synthesis and production [1-2]. SAR images have shown potential for separating tree species in all-weather, day or night conditions, at a high spatial resolution, but most studies have been limited to the analysis of scatter plots [3], or color images [4], and very few attempts have actually been made to map species composition on a pixel to pixel basis and estimate the number of pixels correctly classified. In addition, establishing relationships between radar signatures and forest parameters is still an active area of research [5], so that identifying tree species from SAR data alone, without requiring ground-truth verification, is difficult. Finally, mapping species composition using remote sensing techniques may only apply to a limited range of tree structure and environmental conditions, and those limitations need to be determined.

In this paper, we present Classification results obtained from multi-date, multi-channel, airborne SAR observations of Alaskan boreal forests. A maximum a posteriori Bayesian classifier is used to perform a supervised classification of tree species, and evaluate the added value of various polarizations and frequencies for improving classification accuracy, as well as the effect of environmental conditions on the mapping capability of SAR. The results are compared with those obtained using spaceborne observations at optical wavelengths from the Satellite Pour l'Observation de la Terre, SPOT. Finally, we briefly discuss the inference of above ground woody biomass from SAR data, its dependence on species composition and on environmental conditions; and how SAR and SPOT combined help identify species composition independent of ground truth verification and provide input ecological parameters of interest to models of atmosphere-biosphere CO₂ exchange.

SPECIES COMPOSITION FROM SAR

A Maximum A Posteriori Bayesian classifier for multifrequency polarimetric SAR data [6] is used to perform a supervised classification of six categories of terrain Cover: 1) white spruce; 2) black spruce; 3) balsam poplar; 4) alder; 5) treeless areas; and 6) open water. SAR observations of the Bonanza Creek Experimental forest (64° 45'N, - 148°W) were collected on 3 different dates in March 1988, during which the forest changed from frozen to thawed conditions and back to frozen conditions due to a transition to unusually warm temperatures [7], and on 3 different dates in May 1991, during which the forest changed from flooded conditions to unflooded conditions with the receding of the Tanana river waters [8]. In 1988, P-band was only available on March 13, and C-band was corrupted on March 13. In 1991, all frequencies were available but P-band was corrupted on several dates. The multi-date SAR scenes were all co-registered to May 6, 1991 scene. A total of 59 polygonal training sites were selected in the 10 km² region along the Tanana river for which species composition was known from ground truth verification. 22 of these stands were used to compute the mean radiometric and polarimetric characteristics of the six identified terrain categories, which were then used as input parameters for the classifier. Classification accuracy (the number of correctly classified pixels divided by the total number of pixels) was computed for all 59 stands and recorded in confusion matrices (Table 1-8).

The highest classification accuracy is obtained using L- and C-band fully polarimetric on May 6, 1991, where the forest is just recovering from river flooding. 86% of the forest pixels are correctly classified, and 91% overall (i.e. including open water) (Table 1). A digital vegetation map assembled from infra-red aerial photos by USGS EROS Alaska Field Office, Anchorage, Alaska yields 73% classification accuracy for the forest pixels and 89% overall (Table 2) because it does not include treeless areas created by clear-cutting of trees and forest fires between 1978, date of acquisition of the infra-red photos, and 1991. Excluding the treeless areas, the vegetation map has only a 87% accuracy, because several tree stands were incorrectly labeled or probably changed in nature between 1978 and 1991. Using L-band frequency alone yields an accuracy of only 78% (Table 3). On March 13, 1988, when the forest is in thawed state due to unusually warm temperatures, L- and P-band polarimetric combined have an accuracy of 70% (Table 5). On March 19, 1988, when the forest is in frozen state, the accuracy is only 44% (Table 6). Data acquired at the peak of flooding on May 3, 1991 yield accuracies 10% lower than those obtained on May 6, 1991 because strong tree-trunk/ground interactions mask out finer differences in radar backscatter between tree species on May 3. Combination of several of these dates does not improve classification accuracy.

On a single date, C-band and HV-polarization are, respectively, the most useful frequency and polarization for tree mapping (Fig. 1, and Table 4). C-band HV probably is mostly due to scattering from branches and reveals differences in branch geometry and foliar biomass, while L-band HV probably reveals differences in above ground woody biomass, i.e. including branches and trunks. C-band VV (JRS-1 mode), L-band HH (J-J-1 {S-1 mode}), and C-band HH (RADARSAT mode) combined yield

areasonable accuracy (Table 7), while each one of them alone yields poor accuracies. C-band HH in particular provides a good discrimination of willow, alder and balsam poplar probably because trunk-ground interactions are more important in alder trees which are closer to the river and are still flooded, while balsam poplar trees are away from the river bank, at higher elevations, and unflooded on May 6.

SPECIES COMPOSITION FROM SPOT

Multispectral optical data acquired by SPOT on August 8, 1991 were used to classify the same area. Image classes were selected based on a multi-dimensional cluster analysis of visible, red, and infra-red radiances, and classification was performed using a classifier similar to the one used for the SAR data. The classification accuracy (78% for the trees and 90% overall) is lower than that obtained with AIRSAR. SPOT better separates conifers from deciduous trees (different normalized difference vegetation indexes (NDVI)), but does not separate black spruce from white spruce, and alder from balsam poplar (saturated NDVI) (Table 8).

WOODY BIOMASS FROM SAR

The retrieval of biomass from SAR data is investigated using inversion curves derived for maritime pine plantations [5]. The results confirm that the longer wavelengths (L- and P-bands) are best for biomass retrieval, and cross-polarization is better than co-linear polarization. However, environmental conditions strongly affect the performance of the inversion, because of dramatic changes in the water content of the soil and vegetation during freeze/thaw, and drought/flood transitions. The effect is more important at L-band than at P-band (Fig. 3-4). When the trees are frozen, the retrieval of biomass is difficult (Fig. 3). Flooded trees also create a special situation. The best fit between the maritime pine inversion curve and the radar measurements is for the SAR data acquired on May 7, 1991, when the forest is unflooded (Fig. 2). In addition, differences exist between tree species. For instance, black spruce stands have an overestimated biomass level. Black spruce trees are typically smaller in height, but with a higher stem density compared to maritime pine trees [5]. Small and dense trees can have the same biomass level as tall and sparse trees and yet exhibit different radar backscatter values. Differences in tree geometry (e.g. distribution of branches) could also be a factor. Nevertheless, when the forest is neither flooded nor frozen, the inversion curve from maritime pine plantations helps separate areas of no biomass, low biomass (1 ton/ha), intermediate biomass (10 to 100 tons/ha), and high biomass (>150 tons/ha) in the natural forests of Alaska. For comparison, NDVI computed from SPOT data show no correlation with above ground biomass (Fig. 5), as in [9].

SYNERGISTIC USE OF SAR AND OPTICAL

Combining SPOT and SAR helps identify tree species, independent of ground truth verification, a step that should be ultimately achieved using only one sensor. In the summer, NDVI separates deciduous trees (balsam poplar and alder) from conifers (white spruce and black spruce), treeless areas covered by a short vegetation of shrubs (clear-cuts, recently burned areas), and open water (Fig. 5); whereas SAR data at L-band HV-polarization provide 4 different levels of biomass, corresponding to no biomass (open water), treeless areas (clear-cuts), intermediate biomass (black spruce and alder), and high biomass (white spruce, and balsam poplar) (Fig. 2). A segmentation map from multi-channel SAR data could provide groups of image pixels that are naturally separated by the radar and that have homogeneous and similar radiometric and polarimetric characteristics. The labeling of each group into a tree type based on its biomass level estimated from SAR and its NDVI from SPOT would then yield

a map of species composition. Knowing the NDVI of the different stands provides information about leaf area index (LAI), which, combined with species composition, yield key parameters for modeling atmosphere-biosphere CO₂ exchange [1].

CONCLUSIONS

The results show that SAR can map tree species of Boreal forest with a high classification accuracy, comparable to that obtained with optical sensors, and to that obtained from vegetation maps assembled from digitized aerial photos that typically require several years for completion. In the Arctic, where cloud cover is relatively important, SAR has a definite advantage. The mapping capability of SAR is poor in winter when the trees are frozen, and during spring break up when the trees are flooded. Multi-date imagery does not help improve classification and even degrades it significantly. By reducing the number of channels used for classification we evaluated in a quantitative fashion the added value of various frequencies and polarizations. The effect of environmental conditions and of tree species on the inference of forest parameters from SAR data was investigated, showing that frozen and flooded conditions yield difficult situations for the inversion. In future studies, we will address the potential for SAR to map tree species in the presence of topography since topographic maps registered with the SAR data are now available in operational mode aboard AIRSAR. More work is also needed to develop an automated mapping capability using SAR alone by improving our current knowledge of the relationships between SAR signatures and forest parameters other than biomass.

ACKNOWLEDGEMENTS This work was carried out at the Jet Propulsion Laboratory, California Institute of Technology, under contract with the National Aeronautics and Space Administration.

REFERENCES

- [1] Bonan G., Importance of leaf area index and forest type when estimating photo-synthesis in Boreal forests, *Int. J. Remote Sensing*, 1993.
- [2] Kasishke E. S., and N. L. Christensen, Connecting forest ecosystem and microwave backscatter models, *Int. J. Remote Sensing* 11, 1277-1295, 1990.
- [3] Sieber A. J., Forest signatures in imaging and non-imaging microwave scatterometer data, *ESA J.*, 431.448, 1985.
- [4] Cimino J. II., A. Brandani, D. Casey, J. Rabassa, and S. Wall, Multiple incidence angle Silt-11 experiment over Argentina: Mapping of forest units, *IEEE Trans. Geosc. and Rem. Sens.* 24, 49 S-509, 1986.
- [5] LeToan T., A. Beaudoin, J. Rioux, and D. Guyon, Relating forest biomass to SAR data, *IEEE Trans. on Geosc. and Rem. Sens.* 30, 403-411, 1992.
- [6] Rignot E., and R. Chellappa, Segmentation of polarimetric synthetic aperture radar data, *IEEE Trans. on Image Proc.*, 1, 281-300, 1992.
- [7] Way, J. B. and 15 others, The effect of changing environmental conditions on microwave signatures of forest ecosystems: preliminary results of the March 1988 Alaskan aircraft SAR experiment, *Int. J. Remote Sensing* 11, 1119-1144, 1990.
- [8] McDonald L. J., J. B. Way, E. Rignot, C. Williams, L. Viereck, and P. Adams, Monitoring environmental state of Alaskan forests with AIRSAR, *Proc. Third Ann. J. Airborne Geosc. Workshop* 3, J. van Zyl, Ed., 7-8, 1992.
- [9] Sader S. A., Forest biomass, canopy structure, and species composition relationships with multipolarization L-band synthetic aperture radar data, *Photogramm. Eng. and Rem. Sens.* 53, 193-202, 1987.

1							2						
Tree Type	CC	AL	BP	WS	HS	Water	Tree Type	CC	AL	BP	WS	HS	Water
CC	78	0	0	0	0	0	CC	0	2	1	0	0	4
AL	0	80	0	0	0	0	AL	0	79	4	0	0	1
BP	0	17	88	15	0	0	BP	0	7	82	2	0	0
WS	0	3	6	84	10	0	WS	95	0	3	93	4	1
HS	21	0	0	0	1	87	HS	0	0	0	0	88	0
Wa	0	0	0	0	0	100	Wa	5	12	0	5	8	95

3							4						
Tree Type	CC	AL	BP	WS	HS	Water	Tree Type	CC	AL	BP	WS	HS	Water
CC	66	0	0	0	1	0	CC	55	0	0	0	2	0
AL	0	15	0	21	0	0	AL	0	61	34	2	0	10
BP	0	38	96	21	0	0	BP	0	39	57	6	1	0
WS	33	46	4	51	8	0	WS	1	0	7	81	24	0
HS	33	0	0	1	no	0	HS	16	0	2	11	72	0
Wa	0	0	0	0	0	100	Wa	27	0	0	0	0	100

5							6						
Tree Type	CC	AL	BP	WS	HS	Water	Tree Type	CC	AL	BP	WS	HS	Water
CC	79	3	1	0	3	2	CC	73	22	4	1	32	1
AL	2	75	14	6	23	0	AL	6	17	19	5	8	0
BP	1	8	77	38	2	0	BP	3	4	20	10	4	0
WS	1	5	5	53	7	0	WS	3	2	39	69	13	0
HS	17	9	3	3	65	0	HS	14	15	18	15	43	0
Wa	0	0	0	0	0	98	Wa	0	42	0	0	0	99

7							8						
Tree Type	CC	AL	BP	WS	HS	Water	Tree Type	CC	AL	BP	WS	HS	Water
CC	91	0	0	0	1	0	CC	88	0	0	0	0	1
AL	0	66	17	1	1	0	AL	0	40	8	0	0	0
BP	0	33	71	13	2	0	BP	2	51	78	4	6	0
WS	1	1	10	84	20	0	WS	0	0	5	93	25	0
HS	8	0	3	2	77	0	HS	1	0	0	2	69	0
Wa	0	0	0	0	0	100	Wa	9	0	0	1	0	99

Tables Confusion matrices for (1) L- and C-band fully polarimetric on May 6, 1991. Total classification accuracy is 90.8%; and 86.2% for trees only. (2) Digital vegetation map. Total classification accuracy is 89.3%; and 72.8% for trees only. (3) L-band fully polarimetric on May 6, 1991. Total classification accuracy is 78.2%; and 69.7% for trees only. (4) C-band fully polarimetric on May 6, 1991. Total classification accuracy is 84.5%; and 71.77% for trees only. (5) L- and P-band fully polarimetric, on March 13, 1988. (6) L- and C-band fully polarimetric, on March 19, 1988. (7) L-band HH, C-band VV, and C-band HH data on May 6, 1991. Total classification accuracy is 88.0%; and 81.5% for trees only. (8) Multispectral SIOI data acquired on August 28, 1991. Total classification accuracy is 90.1%; and 77.8% for trees only.

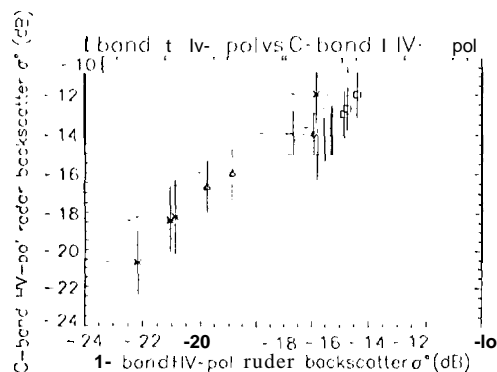


Figure 1. Radar backscatter σ_{HV}^L at L-band HV-polarization on May 6, 1991 versus σ_{HV}^C at C-band HV-polarization. Treeless areas (*), black spruce (A), alder (x), white spruce/balsam poplar (3), balsam poplar (2), and white spruce (4).

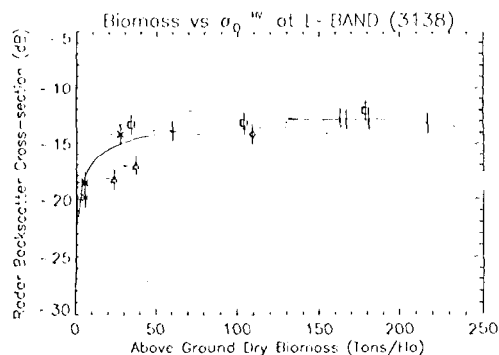


Figure 2. Radar backscatter σ_{HV}^L at L-band HV-polarization on May 7, 1991 versus the above ground woody biomass. The continuous line is adapted from the maritime pine inversion curve [5]. Error bars correspond to the standard deviation of the measurements in each stand for the biomass and the σ_{HV}^L values.

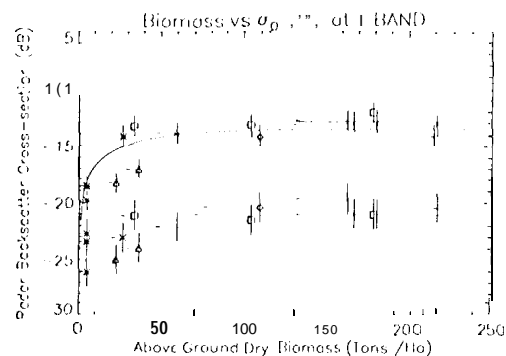


Figure 3. Radar backscatter σ_{HV}^L at L-band HV-polarization on 4 different dates (March 13, 1988; March 19, 1988; May 3, 1991; and May 7, 1991) versus the above ground woody biomass (tons/ha).

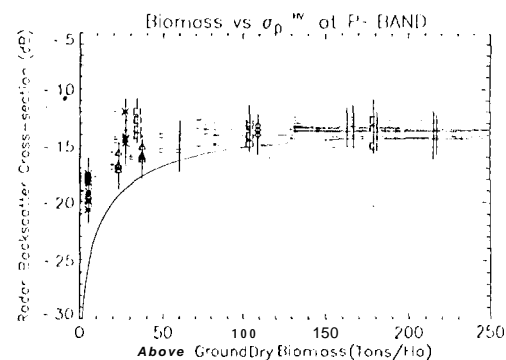


Figure 4. Radar backscatter σ_{HV}^P at P-band HV-polarization on 4 different dates (March 13, 1988; March 19, 1988; May 3, 1991; and May 7, 1991) versus the above ground woody biomass (tons/ha). The continuous line is an adapted version of the maritime pine inversion curve [5].

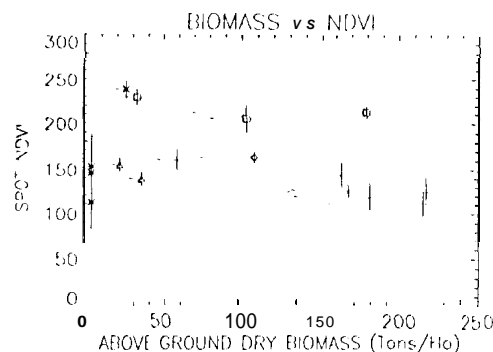


Figure 5. NDVI indexes from SIOI data versus the above ground woody biomass (tons/ha).